第6回特定・宇宙ニュートリノ研究会

太陽ニュートリノの教養物理

南才 久和
(都立大・RCCN)

太陽ニュートリノの謎

太陽は光だけではなくニュートリノを放出している！

☺ 太陽は核融合反応をそのエネルギー源として輝いている。

主な核反応：

$$p + p + p + p \longrightarrow {}^4He + 2e^+ + 2\nu_e$$

地上でのニュートリノ・フラックス：超い評価

$$F = 2 \times \left(\frac{\text{太陽のルミノシティ}}{{}^4He\text{の束ばくエネルギー}} \right) \times \frac{1}{4\pi R_{AU}^2}$$

（太陽のルミノシティ：$\sim 10^{38}\ s^{-1}$ erg/s）

（${}^4He$の束ばくエネルギー：1回の反応で出るエネルギー）

（R_{AU}：太陽－地球間距離）

$$= 2 \times \frac{4 \times 10^{33}\ erg/s}{28\ MeV \cdot 4\pi \left(1.5 \times 10^{13}\ cm\right)^2}$$

$$\simeq 6 \times 10^{10}\ cm^{-2} \cdot s^{-1} \qquad \left(1\ MeV = 1.6 \times 10^{-6}\ erg\right)$$

Nuclear reactions in the pp-chain

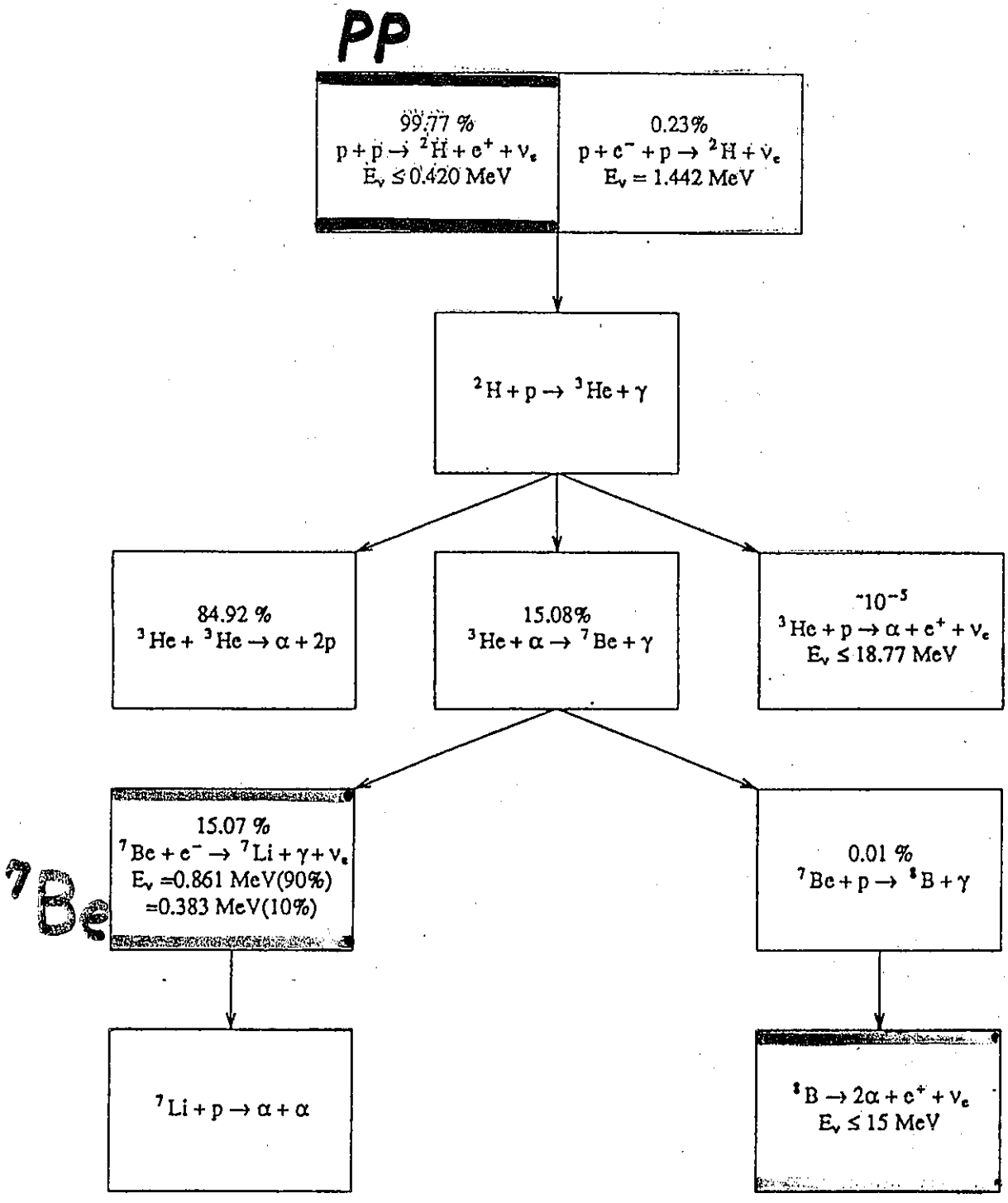

Figure 1.1. Nuclear fusion reaction sequences in the Sun [ref. 1.4]

No.

Date

pp I Chain

$p + p \longrightarrow {}^2H + e^+ + \nu_e$

$p + p \longrightarrow {}^2H + e^+ + \nu_e$

${}^2H + p \longrightarrow {}^3He + \gamma$

${}^2H + p \longrightarrow {}^3He + \gamma$ Termination

${}^3He + {}^3He \longrightarrow {}^4He + 2p$ (85%)

$p + p + p + p \longrightarrow {}^4He + 2e^+ + 2\nu_e\,(pp) + \gamma$'s

pp II Chain

$p + p \longrightarrow {}^2H + e^+ + \nu_e$

${}^2H + p \longrightarrow {}^3He + \gamma$

${}^3He + {}^4He \longrightarrow {}^7Be + \gamma$ (15%)

${}^7Be + e^- \longrightarrow {}^7Li + \nu_e$

${}^7Li + p \longrightarrow 2\,{}^4He$

$p + p + p + p + e^- \longrightarrow {}^4He + e^+ + \nu_e\,(pp) + \nu_e\,({}^7Be) + \gamma$'s

No.

Date

pp III Chain

$$p + p \longrightarrow {}^2H + e^+ + \nu_e$$

$${}^2H + p \longrightarrow {}^3He + \gamma$$

$${}^3He + {}^4He \longrightarrow {}^7Be + \gamma$$

$${}^7Be + p \longrightarrow {}^8B + \gamma \qquad (0.02\%)$$

$${}^8B \longrightarrow {}^8Be^* + e^+ + \nu_e$$

$${}^8Be^* \longrightarrow 2\,{}^4He$$

$$p + p + p + p \longrightarrow {}^4He + 2e^+ + \nu_e(pp) + \nu_e({}^8B) + \gamma's$$

標準太陽模型によって予言されるニュートリノ・スペクトル

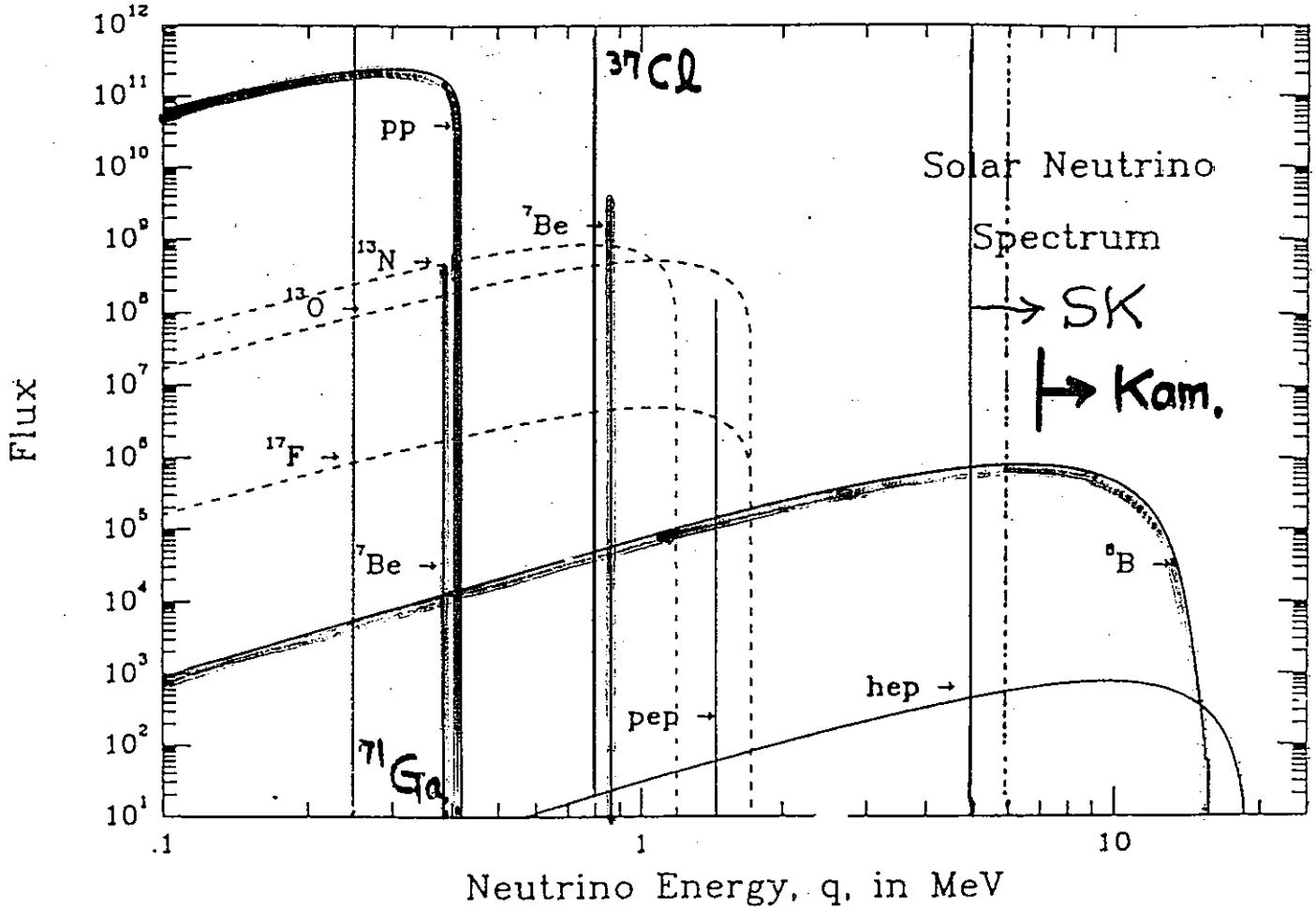

FIG. 2. The solar neutrino energy spectrum predicted by the Standard Solar Model

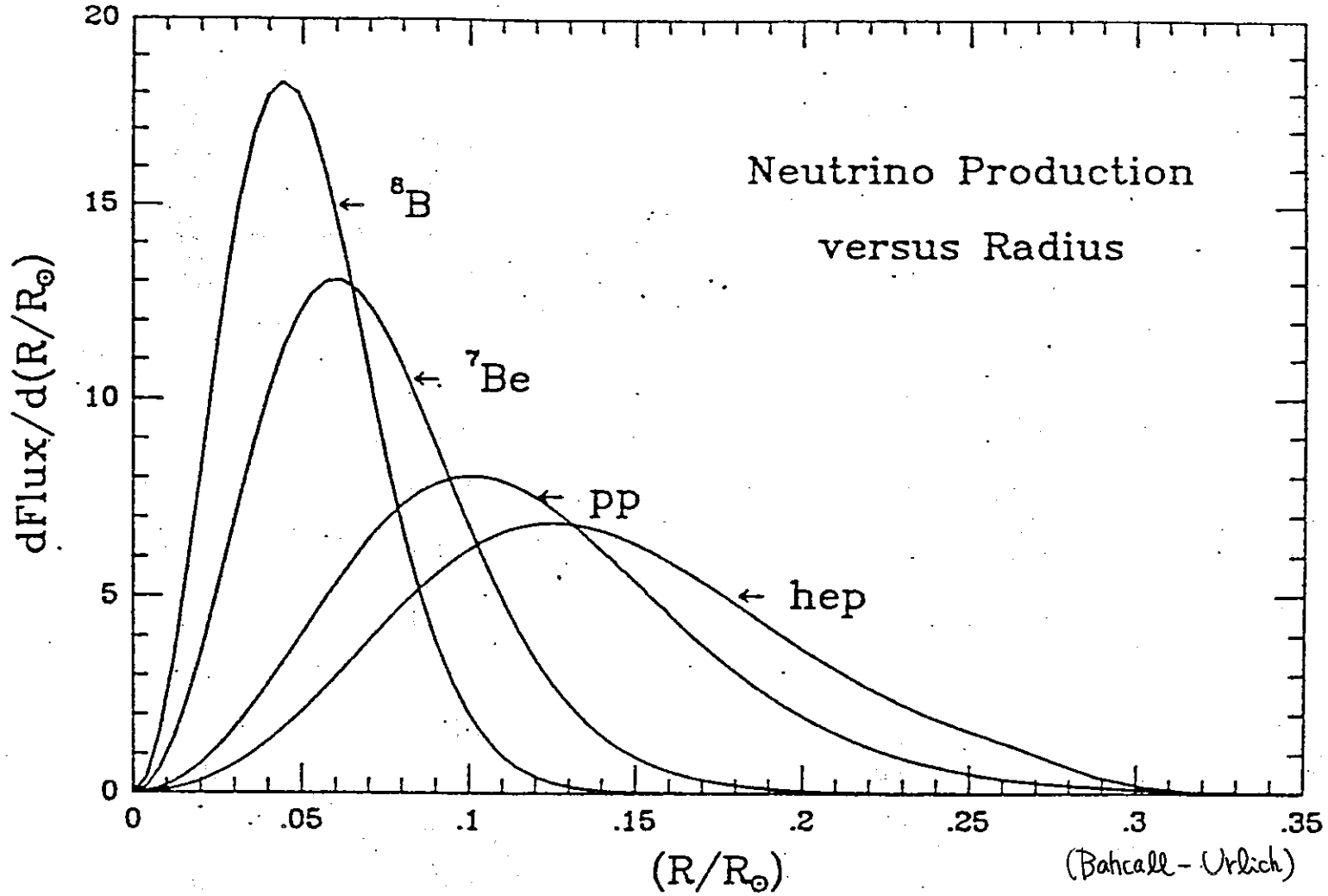

FIG. 8. Neutrino production as a function of radius. The fraction of neutrinos that originate in each fraction of the solar radius is $[d\,\mathrm{Flux}/d(R/R_\odot)][d(R/R_\odot)]$. The figure illustrates the production fraction for ^{8}B, ^{7}Be, *p*-*p*, and hep neutrinos for the standard solar model described in Sec. V.B and Table XI.

solar
have c
tions u
model,
action
in Tal
model
tion 6
for rea
I); the
often a
The
moder
The
34%.
this flu
nuclea
thougl
heavy-

① Hydrostatic Equilibrium

$$\frac{dP(r)}{dr} = -\frac{GM(r)}{r^2}\rho(r)$$

$$P(r) = \frac{k}{\mu m_p}\rho T + \frac{1}{3}aT^4$$

gas pressure $\gg$ radiation pressure

[At $r=r_{1/10}$ $\sim 8\times10^{19}\left(\frac{J}{m^3}\right) \gg \sim 6\times10^{12}\left(\frac{J}{m^3}\right)$]

$M(r_{1/10}) \approx \frac{1}{10}M_\odot$ μ = mean molecular weight

<note>

$$\mu = \frac{\sum_i n_i A_i}{n_e + \sum_i n_i} \simeq \frac{1}{2X + \frac{3}{4}Y + \frac{1}{2}(1-X-Y)}$$

mass fraction of: Hydrogen, He, heavy elements

② Energy Generation

$$\frac{d}{dr} L(r) = 4\pi r^2 \rho(r) \varepsilon(r)$$

$L(r)$: Luminosity at radius r ($J \cdot s^{-1}$)

$\varepsilon(r)$: energy generation rate at radius r ($J\, s^{-1} kg^{-1}$)

$$\rho(r)\varepsilon(r) = \sum_{i,j} (Q - q_\nu) \langle \sigma v \rangle$$

$\langle \sigma v \rangle$: average over thermal velocity

$$\langle \sigma v \rangle = \left(\frac{8}{\pi \mu (kT)^3} \right)^{1/2} f_0 \int_0^\infty dE \, \boxed{S(E)} \exp\left(-2\pi\eta - \frac{E}{kT} \right)$$

f_0: screening factor due to screening

$S(E)$: astrophysical S factor

$$\sigma(E) = \frac{\boxed{S(E)}}{E} e^{-2\pi\eta}$$

$e^{-2\pi\eta}$: Gamow penetration factor

$$\eta = Z_1 Z_2 \frac{e^2}{\hbar v}$$

③ Temperature Profile from Radiative Transfer

energy flux

$$F = -\frac{c}{\kappa\rho}\frac{d}{dr}P_r$$

Rosseland mean absorption coefficient

$$\begin{cases} F = \dfrac{L(r)}{4\pi r^2} \\ P_r = \dfrac{1}{3}aT^4 \end{cases}$$

⊕

$$\frac{1}{r^2}\frac{d}{dr}(r^2F) = \varepsilon\rho \quad : \text{energy conservation}$$

$$\Rightarrow \quad \frac{dT}{dr} = -\left(\frac{3}{16\pi}\right)\frac{\kappa\rho}{aT^3cr^2}L(r)$$

$$a = 7.56 \times 10^{-16} \quad J\,m^{-3}\,K^{-4}$$

Ref. S. Chandrasekhar
An Introduction to the Study of Stellar Structure (Dover 1939)

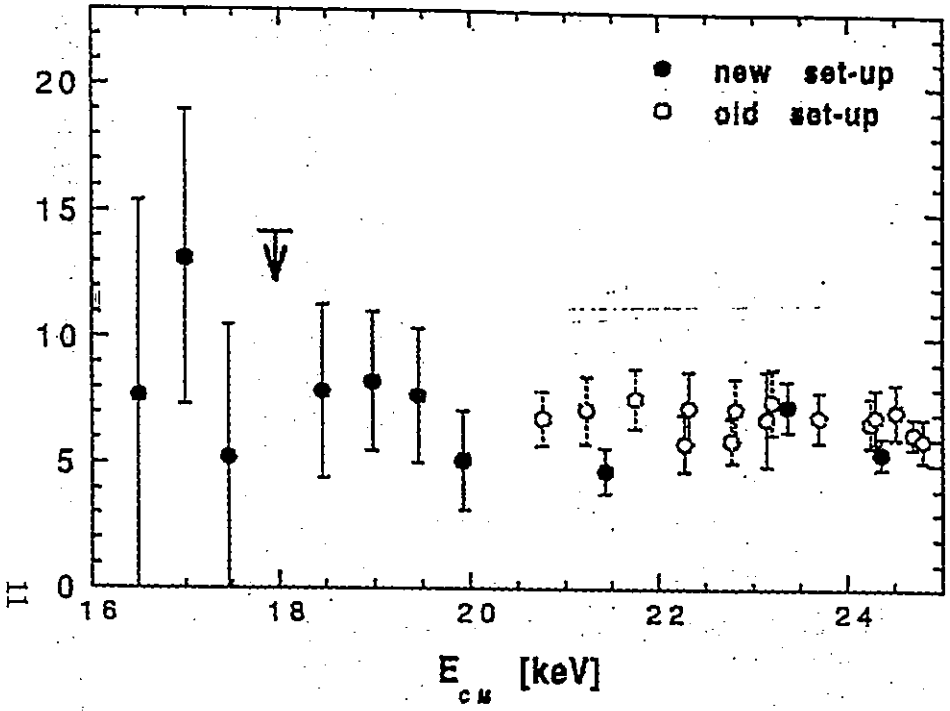

1. The ^{3}He(^{3}He, $2p$)^{4}He astrophysical factor $S(E)$ mea- underground with the LUNA old setup [10] and with the one. The error bars correspond to one standard deviation.

letectors are rejected in order to remove the residual onic noise and the muon induced showers.
ese requirements lead to a detection efficiency of ± 0.2)% as determined by the Monte Carlo program
The error comes mainly from the uncertainties on osition of the detectors and on the profile of the beam.

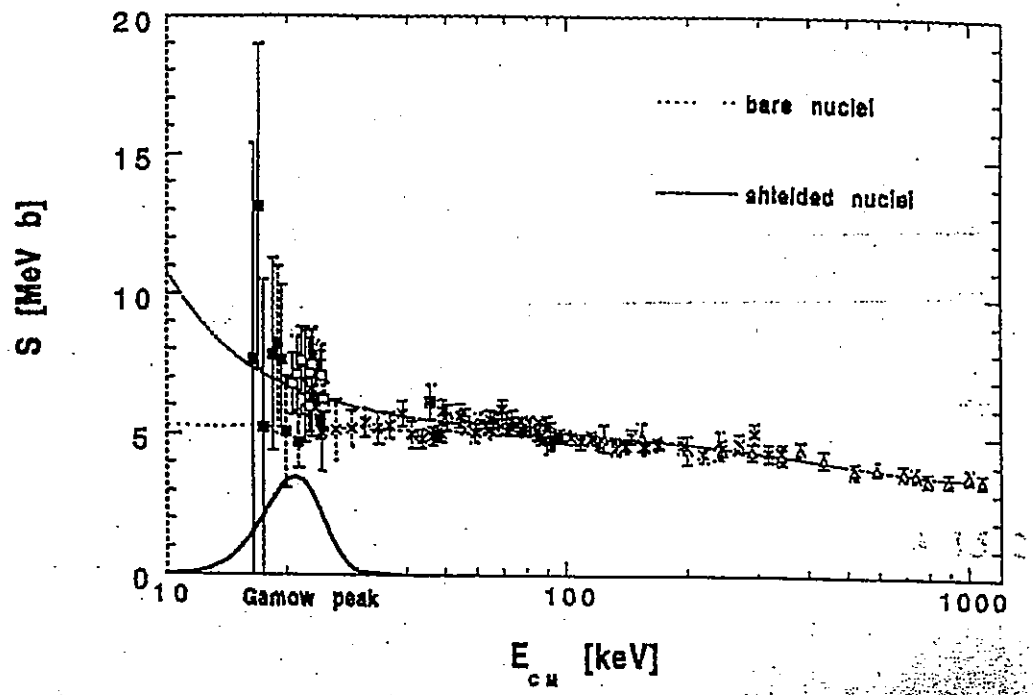

FIG. 2. The ^{3}He(^{3}He, $2p$)^{4}He astrophysical factor $S(E)$ from two previous measurements and from LUNA. The results are from Dwarakanath and Winkler (triangle) [13], Krauss *et al.* (cross) [8], LUNA underground new setup (black square), LUNA old setup [10], both underground (white square) and at the surface (crossed square). The lines are the fit to the astrophysical factors of bare and shielded nuclei. The solar Gamow peak is shown in arbitrary units.

we obtain the values of the parameters $S_b(0)$, $S'_b(0)$, $S''_b(0)$, and U_e given in Table II (S_b and S_s are the astrophysical factors for bare and shielded nuclei, respec

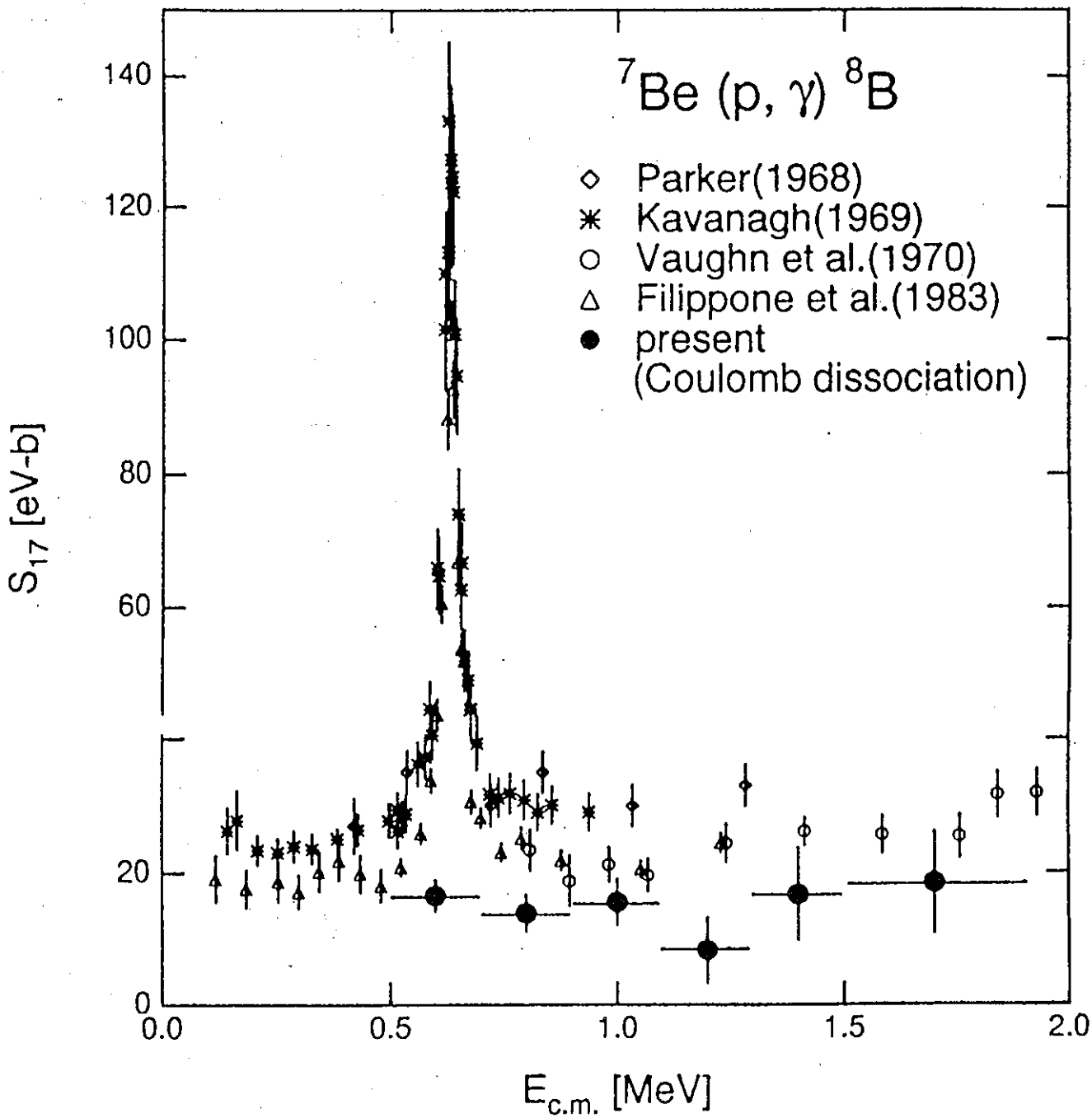

FIG. 3. Comparison of S_{17} extracted from the Coulomb dissociation of ^{8}B and the previous highest precision results. The horizontal bars indicate the range of E_{rel} over which the S factor is averaged.

center-of-mass energy. The Coulomb dissociation results

N. Iwasa et al. J. Phys. Soc. Japan 65 (1996) 1256

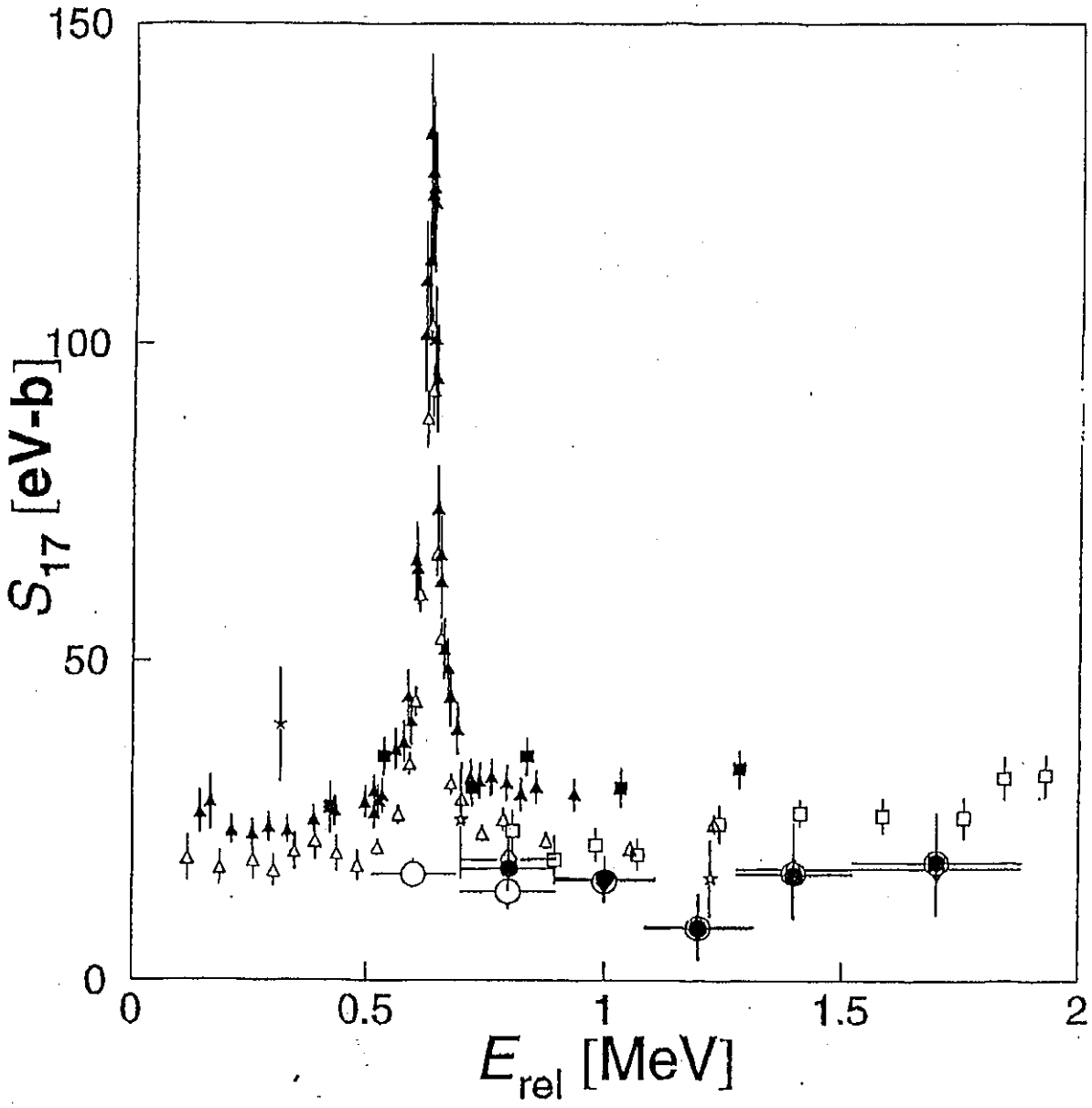

Fig. 5. The astrophysical S_{17}-factors deduced from the present Coulomb dissociation experiment plotted together with existing (p,γ) data renormalized by Filippone (see in the text). The open circles, open diamonds and closed circles represent the results without correction, with correction due to the E2 and M1 mixtures estimated with the model of Kim, Park and Kim and with the same correction with the model of Typel and Baur, respectively (see in the text). Note that the corrected data are not shown at $E_{rel} = 600$ keV, where the M1 resonance dominates and reliable correction to the Coulomb dissociation data is not possible.

N. Iwasa et al., Phys. Rev. Lett. 83 (1999) 2910

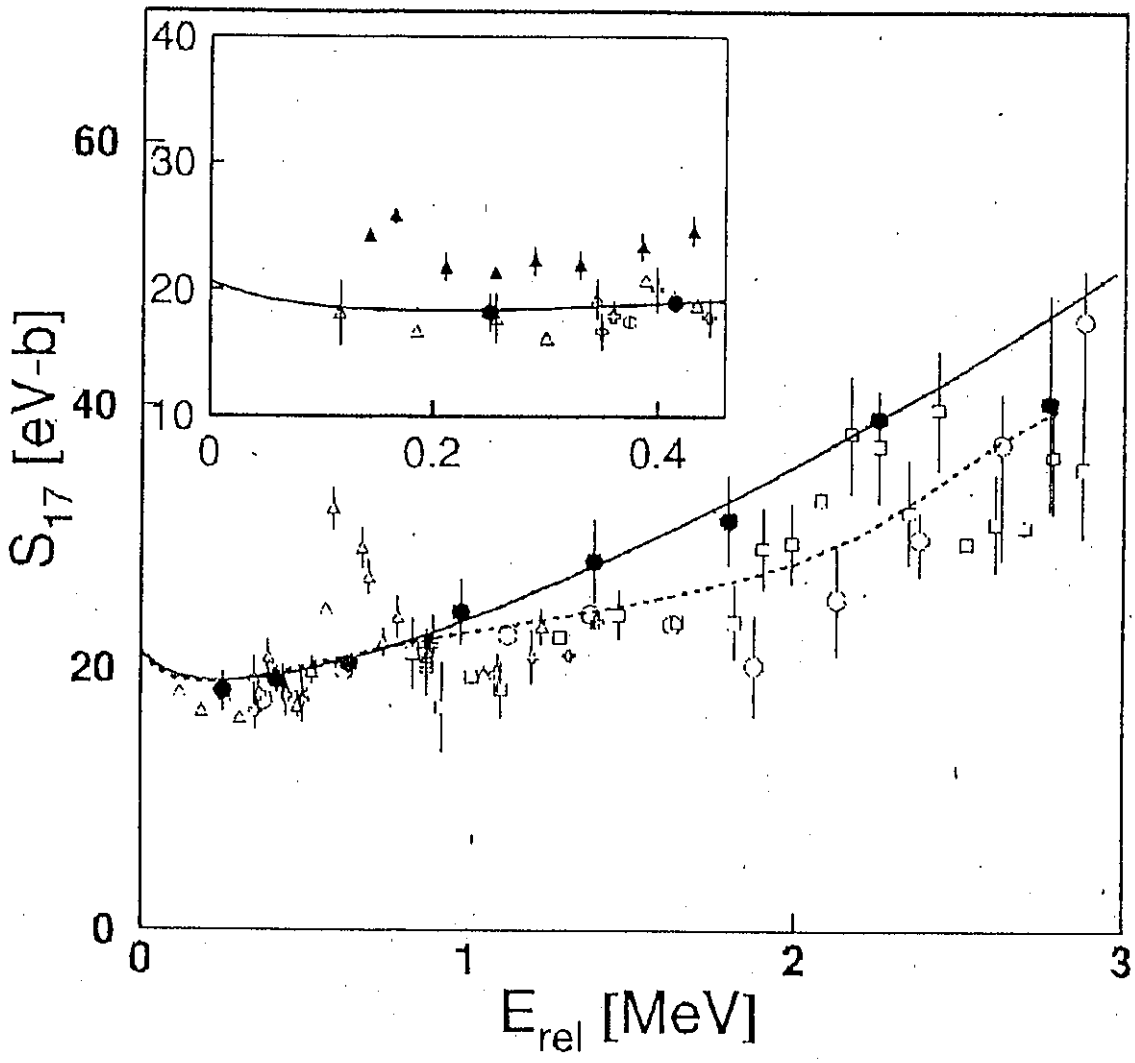

FIG. 3. The astrophysical S_{17}-factors deduced from the present experiment plotted as a function of the p-^{7}Be relative energy (closed circles), in comparison with results from direct and other Coulomb-dissociation experiments (closed triangles from [3], open boxes from [4], open triangles from [5], open crosses from [6], and open circles from [9]). The solid curve shows the prediction of Bertulani [15] fitted to our data, while the dashed curve shows a fit of the theoretical curve of Descouvemont *et al.* [20] to the combined data sets of Refs. [4–6]. The inset shows the low-energy part of the figure, where we have fitted the energy dependence of Jennings *et al.* [24] to our data.

$\nu_\odot$

Global deficit or energy-dependent depletion?

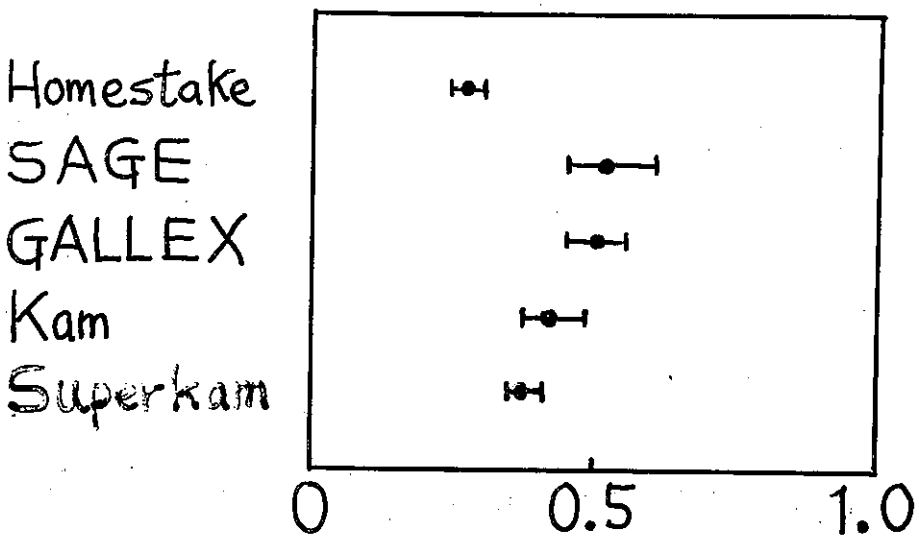

(Totsuka LP97) Data / SSM (BP95)

ted by
adings
of the
ectors.
ninant
in the
by the
tector
o lines
fusion
ure by
oduces
. The
trinos
an see
fluxes
. The
enkov
o have
olds of
URE 2

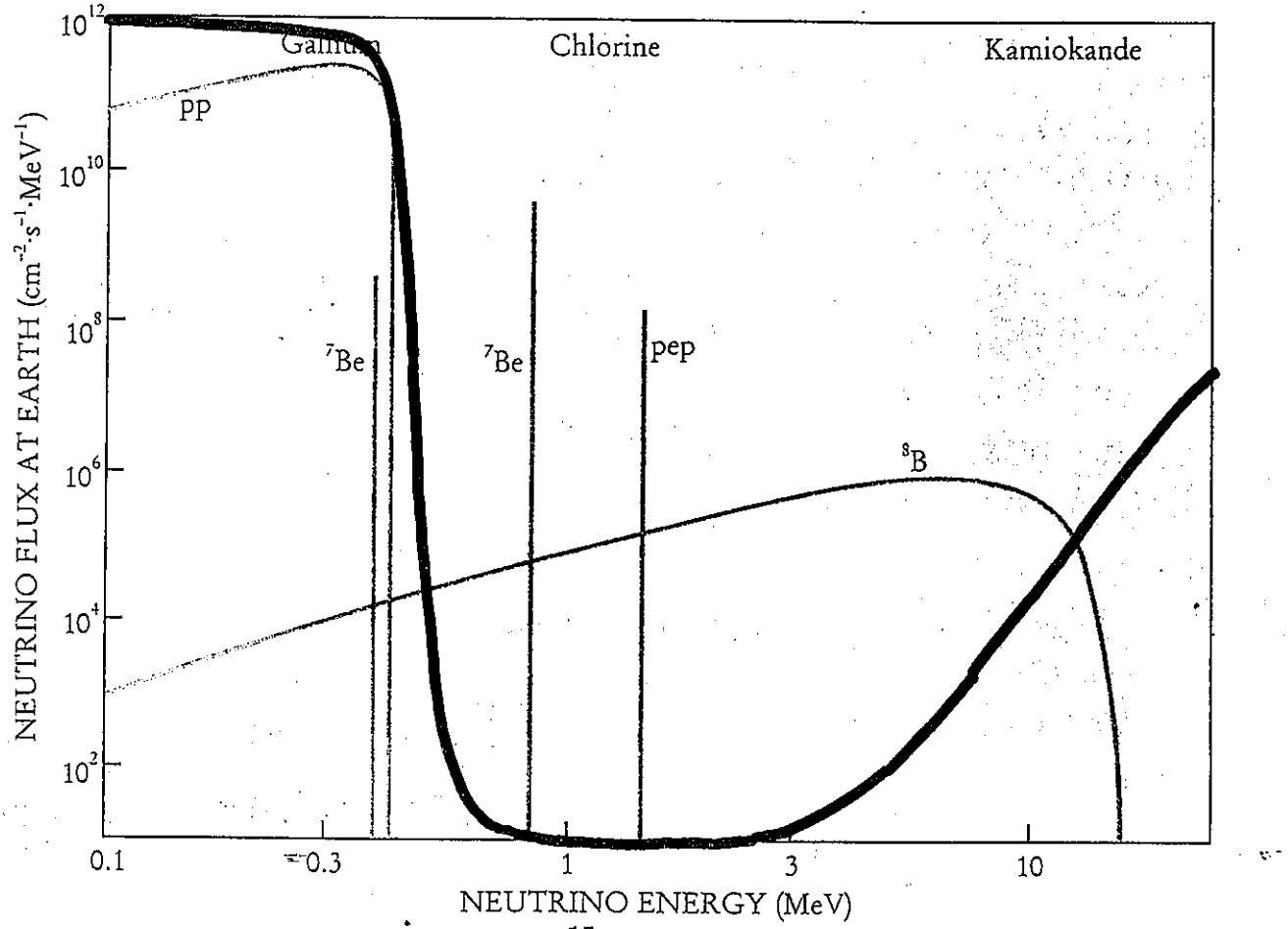

太陽ニュートリノデータの「標準模型によらない」解析

基本仮定

(I) 太陽は核融合反応によって光輝き，ニュートリノはここからのみ発生する。

(II) 太陽中の核反応は標準太陽模型で仮定されているものでつきている。　各反応の相対的な強度比は仮定せず。

(III) 太陽は10万～100万年にわたって準静的。

⇒ Luminosity constraint

Spiro-Vignaud ('90)
Hata-Bludman-Langacker ('94)

Luminosity Constraint

$$L_\odot = \left[Q - 2\langle E \rangle_{pp} \right] \Phi_{ppI} + \left[Q - \langle E \rangle_{Be} - \langle E \rangle_{pp} \right] \Phi_{ppII} + \left[Q - \langle E \rangle_{^8B} - \langle E \rangle_{pp} \right] \Phi_{ppIII}$$

← エネルギー $Q \simeq 26$ MeV を発生する chain が1回 turn した時に発生する γ flux

$$\begin{cases} \Phi(pp) = 2\Phi_{ppI} + \Phi_{ppII} + \Phi_{ppIII} \\ \Phi(^7Be) = \Phi_{ppII}, \qquad \Phi(^8B) = \Phi_{ppIII} \end{cases}$$

→

$$L_\odot = \left[Q - 2\langle E \rangle_{pp} \right] \frac{1}{2} \left[\Phi(pp) - \Phi(^7Be) - \Phi(^8B) \right] + \left[Q - \langle E \rangle_{Be} - \langle E \rangle_{pp} \right] \Phi(^7Be) + \left[Q - \langle E \rangle_{B} - \langle E \rangle_{pp} \right] \Phi(^8B)$$

$$= \sum_{i = pp,\ ^7Be,\ ^8B} \left[\frac{Q}{2} - \langle E \rangle_i \right] \Phi(i)$$

$$\frac{L_\odot}{4\pi R^2} = \sum_i \left[\frac{Q}{2} - \langle E \rangle_i \right] \phi_i$$

($i = pp,\ ^7Be,\ ^8B, \cdots$)

↖ 地球上での γ flux

$$\hat{\phi}_i \equiv \frac{\phi(i)}{\phi(i)_{SSM=BP98}}$$ を定義すると

$$1 = 0.907\,\hat{\phi}_{pp} + 0.0755\,\hat{\phi}_{^7Be} + 4.97\times10^{-5}\,\hat{\phi}_{^8B}$$

$$\begin{pmatrix} \phi(pp)_{BP98} = 5.94\times10^{10} & cm^{-2}s^{-1} \\ \phi(^7Be)_{BP98} = 4.80\times10^{9} & cm^{-2}s^{-1} \\ \phi(^8B)_{BP98} = 5.15\times10^{6} & cm^{-2}s^{-1} \end{pmatrix}$$

⇒ 2d plot !

Expected yields

$$\begin{cases} S_{Cl} = 5.9\,\hat{\phi}_{^8B} + 1.15\,\hat{\phi}_{^7Be} \\ S_{Ga} = 12.4\,\hat{\phi}_{^8B} + 34.4\,\hat{\phi}_{^7Be} + 69.6\,\hat{\phi}_{pp} \\ R_{SK} = \hat{\phi}_{^8B} \end{cases}$$

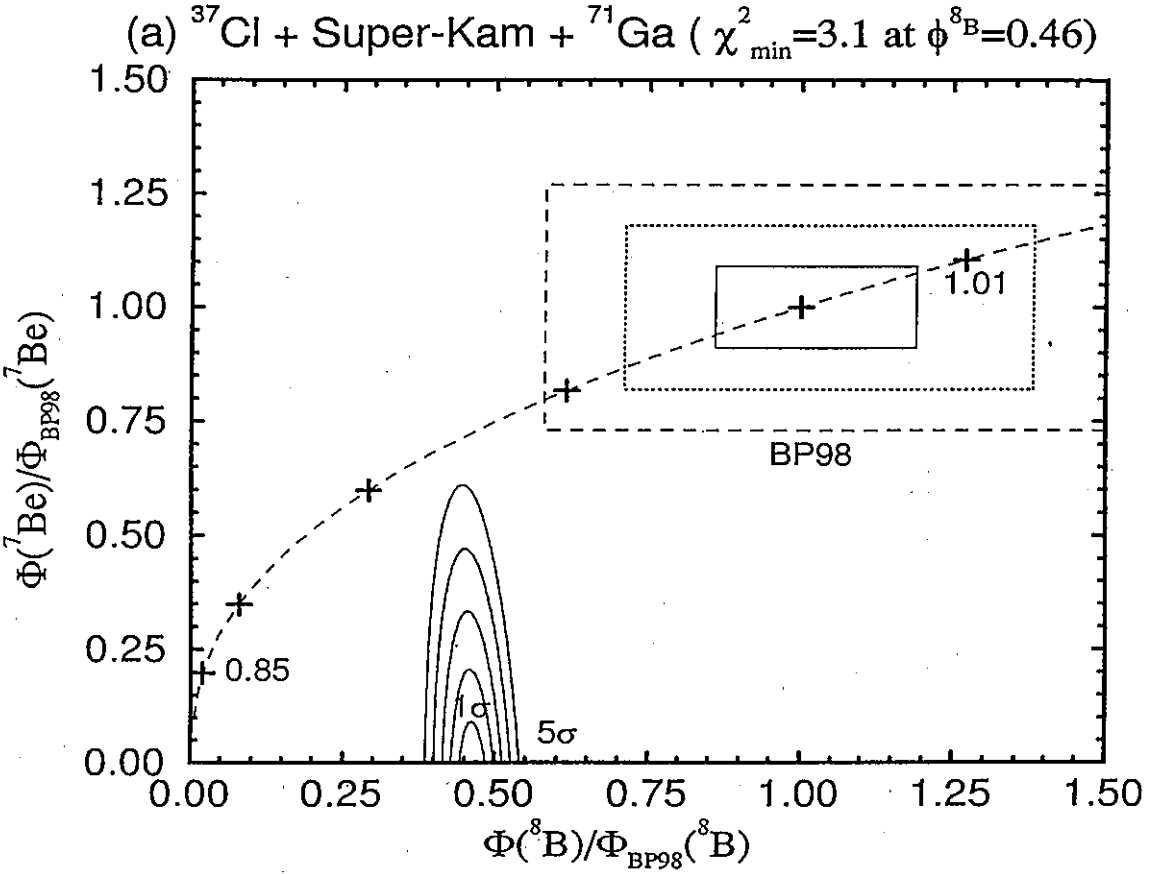

Temperature dependence

$\Phi_{^7Be} \propto T_c^{10}$

$\Phi_{^8B} \propto T_c^{24}$

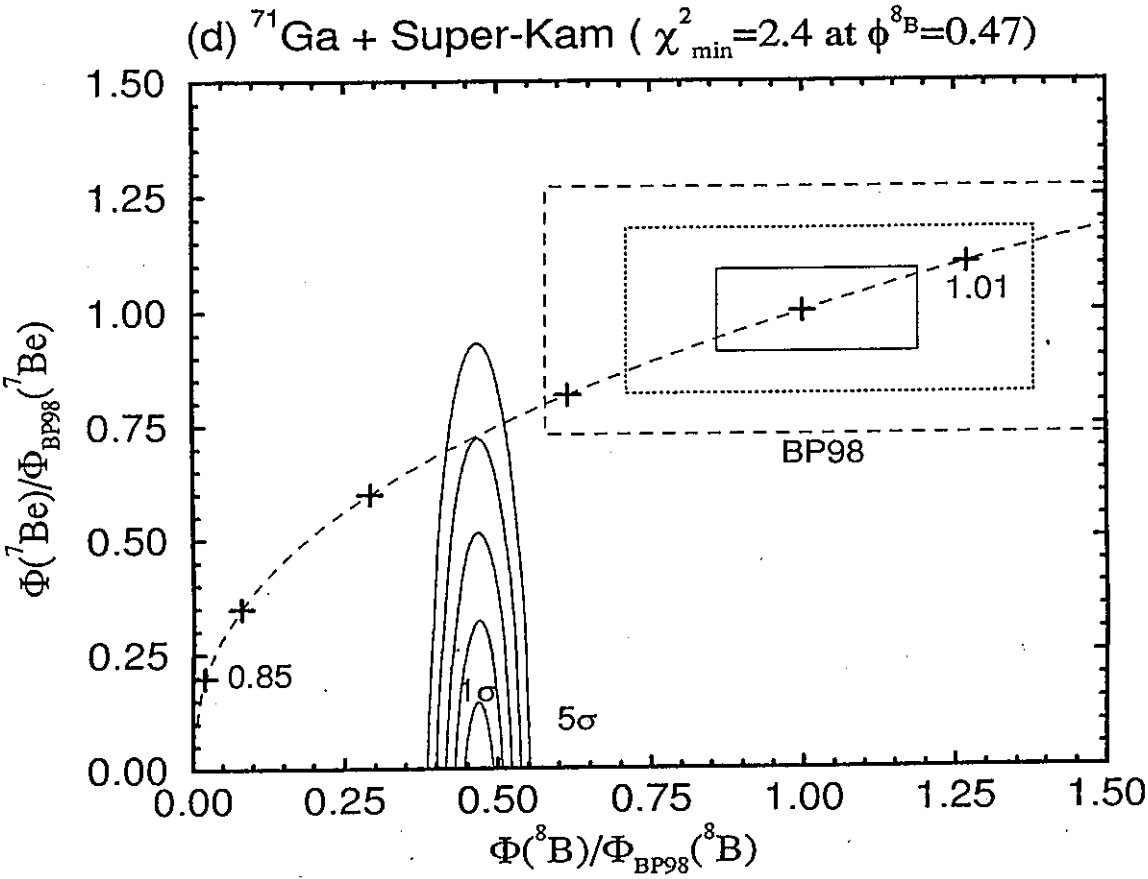
(d) ^{71}Ga + Super-Kam (χ^2_{min}=2.4 at ϕ^{8B}=0.47)
1.50
1.25
1.00
0.75
0.50
0.25
0.00
0.00
0.25
0.50
0.75
1.00
1.25
1.50
$\Phi(^7Be)/\Phi_{BP98}(^7Be)$
$\Phi(^8B)/\Phi_{BP98}(^8B)$
0.85
1.01
BP98
1σ
5σ

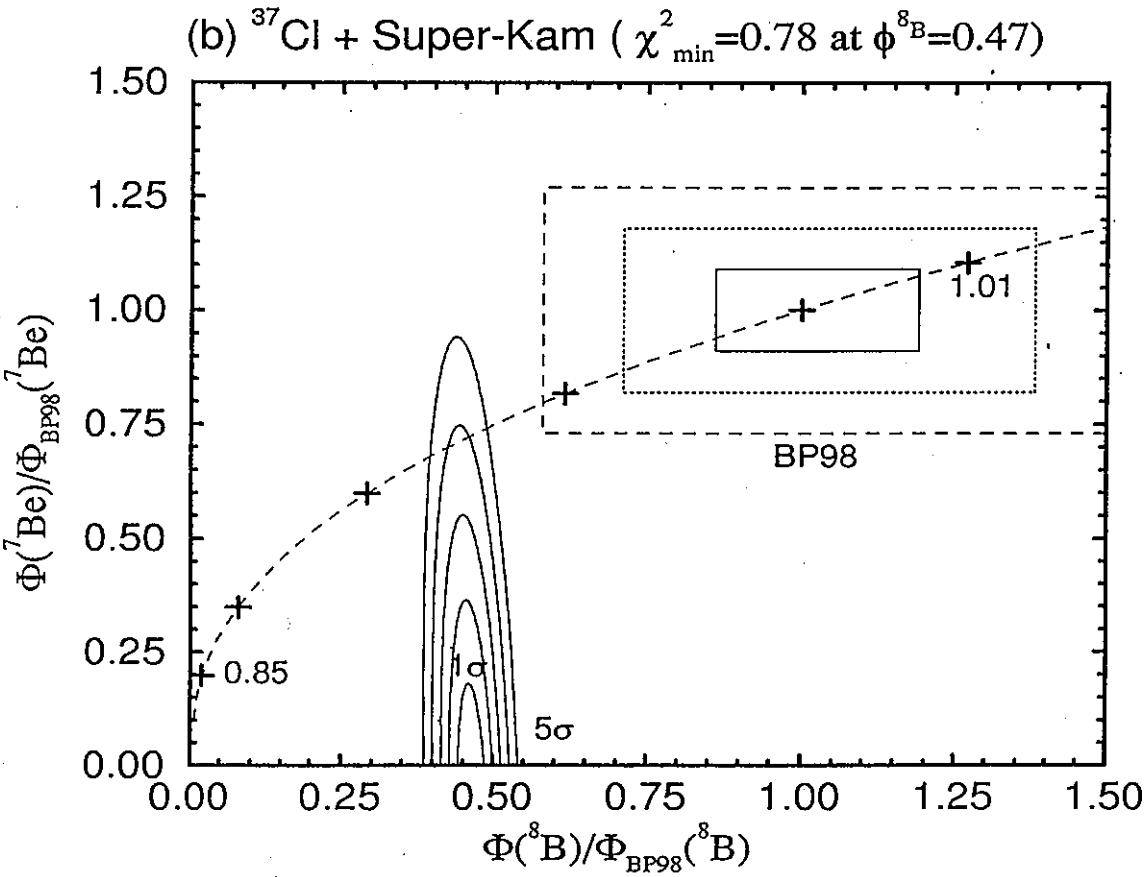
(b) ^{37}Cl + Super-Kam (χ^2_{min}=0.78 at ϕ^{8B}=0.47)
1.50
1.25
1.00
0.75
0.50
0.25
0.00
0.00
0.25
0.50
0.75
1.00
1.25
1.50
$\Phi(^7Be)/\Phi_{BP98}(^7Be)$
$\Phi(^8B)/\Phi_{BP98}(^8B)$
0.85
1.01
BP98
1σ
5σ

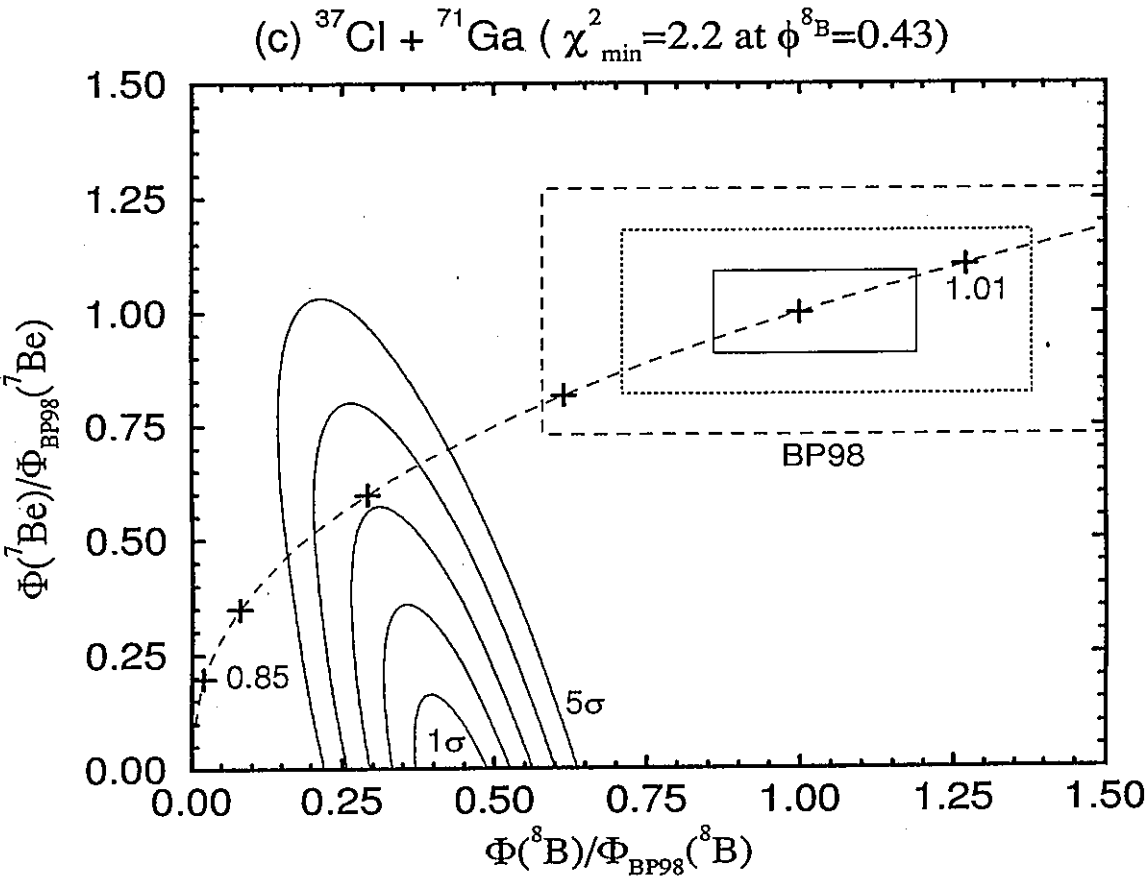
(c) ^{37}Cl + ^{71}Ga (χ^2_{min}=2.2 at $\phi^{^8B}$=0.43)
1.50
1.25
1.00
0.75
0.50
0.25
0.00
0.00
0.25
0.50
0.75
1.00
1.25
1.50
$\Phi(^7Be)/\Phi_{BP98}(^7Be)$
$\Phi(^8B)/\Phi_{BP98}(^8B)$
1.01
BP98
0.85
5σ
1σ